A cosolvent surfactant mechanism affects polymer collapse in miscible good solvents

Swaminath Bharadwaj [1,3]✉, Divya Nayar [1,2,3], Cahit Dalgicdir[1,3] & Nico F. A. van der Vegt [1]✉

The coil–globule transition of aqueous polymers is of profound significance in understanding the structure and function of responsive soft matter. In particular, the remarkable effect of amphiphilic cosolvents (e.g., alcohols) that leads to both swelling and collapse of stimuli-responsive polymers has been hotly debated in the literature, often with contradictory mechanisms proposed. Using molecular dynamics simulations, we herein demonstrate that alcohols reduce the free energy cost of creating a repulsive polymer–solvent interface via a surfactant-like mechanism which surprisingly drives polymer collapse at low alcohol concentrations. This hitherto neglected role of interfacial solvation thermodynamics is common to all coil–globule transitions, and rationalizes the experimentally observed effects of higher alcohols and polymer molecular weight on the coil-to-globule transition of thermoresponsive polymers. Polymer–(co)solvent attractive interactions reinforce or compensate this mechanism and it is this interplay which drives polymer swelling or collapse.

[1] Eduard-Zintl-Institut für Anorganische und Physikalische Chemie, Technische Universität Darmstadt, 64287 Darmstadt, Germany. [2] Centre for Computational and Data Sciences, Indian Institute of Technology Kharagpur, Kharagpur, West Bengal 721302, India. [3] These authors contributed equally: Swaminath Bharadwaj, Divya Nayar, Cahit Dalgicdir. ✉email: bharadwaj@cpc.tu-darmstadt.de; vandervegt@cpc.tu-darmstadt.de

The polymer coil–globule transition is an intramolecular analog of a first order phase transition[1,2]. Various applications of thermoresponsive polymers dissolved in water[3] rely on changes in material properties caused by the coil-to-globule collapse of polymer chains which occurs upon increasing the temperature. The temperature, T(collapse), at which this transition occurs is closely similar to the lower critical solution temperature, LCST, experimentally observed when globular chains aggregate shortly after they collapse[4,5]. Cosolvents, but also salts and small organic molecules (osmolytes) which are typically found in the living cell, affect the LCST and the free energy difference between the coil state and the globule state of various thermoresponsive polymers, such as polyacrylamides[6–11] and elastin-like polypeptides[11,12]. It has been broadly recognized that cosolvents that partition to the polymer surface affect this free energy difference in favor of the coil state, and therefore increase polymer solubility and the LCST. By contrast, cosolvents that are depleted from the polymer surface favor the globule state over the coil state and therefore decrease polymer solubility and the LCST. Although this simple picture applies in many cases, it is not generic and a recent paradigm shift followed several intriguing observations that polymer collapse could in fact be triggered by preferential interactions with cosolvents[13–19], specific salts[20–23], or cosolutes[6,7,24–29] that partition at the polymer surface.

The question we address herein is how these preferential interactions drive polymer collapse in water–alcohol mixtures. Several thermoresponsive polymers undergo coil–globule–coil transitions (cononsolvency) in binary mixtures of two good solvents (e.g., water and alcohol in the case of polyacrylamides) with increasing concentration of the cosolvent (alcohol) at a fixed temperature[4,5,14,17,30–32]. The underlying molecular mechanism is however not understood. Recently reported molecular simulations and theoretical models have emphasized the role of attractive polymer–(co)solvent interactions[5,13–15,33–35], which can be probed in spectroscopy measurements[36,37]. A comprehensive picture is however still missing as it further requires an in-depth understanding of the role of solvent–excluded volume (repulsive) interactions in these systems. While the effect of these repulsive interactions on the polymer coil–globule collapse equilibrium has been discussed previously[16,38,39], conclusive information remains lacking. The solvent–excluded volume contribution to the solvation free energy of a macromolecular solute corresponds to the formation of a repulsive polymer–solvent interface and is determined by the surface tension of the (mixed) solvent[40]. This contribution is not accounted

for in existing polymer theories[34,35,41–45] and cannot be modeled with an effective interaction parameter. Experimentally, its importance is reflected by the fact that the LCST of thermoresponsive polymers correlates with the surface tension increments of the aqueous salt solutions in which they are dissolved[9].

In this work, we report molecular simulations of a generic polymer in water-alcohol mixtures and demonstrate that polymer collapse, which occurs in conjunction with preferential adsorption of amphiphilic alcohol molecules (methanol and ethanol), is driven by changes in the interface formation free energy originating from the above-described repulsive polymer–(co)solvent interactions. We demonstrate that alcohol, added to the solution at low concentration, reduces the interface formation free energy of extended coil-like chains and compact globular chains at different rates, corresponding to faster alcohol saturation and a faster lowering of the free energy of globular chains. This role of interfacial solvation thermodynamics corresponds to a surfactant mechanism driving polymer collapse. It also rationalizes experimentally observed changes in LCST behavior of higher molecular weight polymers[46,47] and changes in LCST behavior in aqueous solutions with higher alcohols[8,19,48].

The surfactant mechanism proposed herein arises from solvent–excluded volume interactions with extended macromolecular surfaces. It should be generic in systems with amphiphilic cosolvents, but maybe offset or reinforced by attractive polymer–(co)solvent interactions.

Results

Polymer collapse free energy. The coil-to-globule ($C \rightarrow G$) collapse free energy, $\Delta G^{C \rightarrow G}$, has been derived from the two-state potential of mean force (PMF), $w(R_g)$, (Supplementary Figs. 1–3) using umbrella sampling with the radius of gyration, R_g, as collective variable (see Methods). Figure 1 shows that the generic polymer exhibits cononsolvency where the radius of gyration R_g of the polymer (inset) and collapse free energy $\Delta G^{C \rightarrow G}$ show a non-monotonic dependence (decrease followed by increase) on the alcohol concentration $X_{Alcohol} = N_{Alcohol}/(N_{Alcohol} + N_{Water})$, where N_{Water} and $N_{Alcohol}$ are the number of water and alcohol molecules in the system, respectively. The minimum in $\Delta G^{C \rightarrow G}$ decreases and shifts to lower alcohol concentration for the higher alcohol (ethanol), in agreement with the cononsolvency behavior of polyacrylamides[8,19,48].

Interestingly, the solvent–excluded-volume contribution to the polymer collapse free energy, $\Delta G^{C \rightarrow G}_{Excl-Vol}$, also shows a non-monotonic dependence on the alcohol concentration (Fig. 1b). This quantity, which corresponds to the difference in the
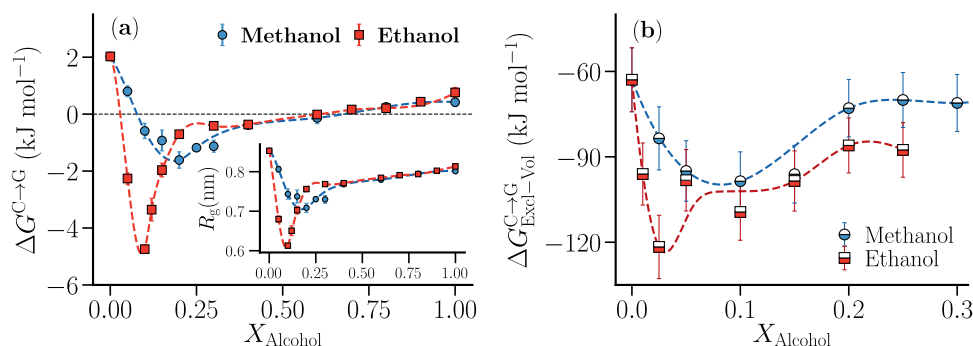
Fig. 1 Polymer collapse free energies in water-alcohol mixtures. Dependence of **a** polymer collapse free energy $\Delta G^{C \rightarrow G}$, radius of gyration R_g (inset) and **b** $\Delta G^{C \rightarrow G}_{Excl-Vol}$ on the alcohol concentration $X_{Alcohol}(= N_{Alcohol}/(N_{Alcohol} + N_{Water}))$. As in the case of polyacrylamides in water–alcohol mixtures[8,19,48], the minimum in $\Delta G^{C \rightarrow G}$ (and R_g) becomes deeper and shifts to lower alcohol concentrations for the higher alcohol. Interestingly, the solvent–excluded-volume contribution, $\Delta G^{C \rightarrow G}_{Excl-Vol}$, also shows the signature of cononsolvency and captures the effect of alcohol size, indicating its important role in driving this phenomenon. Polymer-water and polymer–alcohol Van der Waals interactions were scaled with $\lambda_{pw} = 1.095$ and $\lambda_{pa} = 0.949$, respectively (see Methods). The error bars represent the standard errors in the respective quantities.

reversible work of creating a polymer coil- and a polymer globule-sized cavity in solution, was obtained by thermodynamic integration employing Weeks–Chandler–Andersen (WCA)[49] polymer–water and polymer–alcohol interactions (see Methods). Note that $\Delta G_{\text{Excl}-\text{Vol}}^{\text{C}\rightarrow\text{G}}$ is always negative because polymer cavities with a smaller solvent-accessible-surface area (SASA) impose weaker excluded-volume restrictions on the molecules of the binary solvent. The observed non-monotonic dependence of $\Delta G_{\text{Excl}-\text{Vol}}^{\text{C}\rightarrow\text{G}}$ on the alcohol concentration indicates that solvent–excluded-volume interactions shift the polymer coil–globule equilibrium towards the collapsed globule state upon adding a low alcohol concentration to the solution while shifting it towards the expanded coil state upon adding higher alcohol concentrations. Similar to the trends observed in $\Delta G^{\text{C}\rightarrow\text{G}}$ and R_{g}, the minimum in $\Delta G_{\text{Excl}-\text{Vol}}^{\text{C}\rightarrow\text{G}}$ is deeper and shifts to lower alcohol concentration for the higher alcohol. Since $\Delta G_{\text{Excl}-\text{Vol}}^{\text{C}\rightarrow\text{G}}$ depends only on the solute size and bulk solvent–cosolvent interactions, the results highlight the crucial role played by bulk solvent–cosolvent interactions in driving the cononsolvency phenomenon. The minimum in $\Delta G_{\text{Excl}-\text{Vol}}^{\text{C}\rightarrow\text{G}}$ does not exactly coincide with the minimum in $\Delta G^{\text{C}\rightarrow\text{G}}$ due to the role of attractive polymer–cosolvent interactions in determining the concentration regime of polymer collapse, as discussed later.

Reversible work of cavity creation. The non-monotonic trend observed in $\Delta G_{\text{Excl}-\text{Vol}}^{\text{C}\rightarrow\text{G}}$ correlates with the trends in enthalpy of mixing (ΔH_{mix}) and adiabatic compressibility in pure water-alcohol mixtures as observed in the previous studies[4,8,50]. It has been proposed that adding small amounts of alcohol to a solution of a thermoresponsive polymer in neat water leads to stronger interactions in the bulk solvent which in turn increases the solvation free energy of the coil state thereby causing the polymer to collapse[4,8,44]. If this hypothesis applies, an increase in the reversible work of cavity creation of the coil state ($\Delta G_{\text{Excl}-\text{Vol}}^{\text{C}}$) must be observed with increasing alcohol concentration (at low concentrations) with a larger rate of increase for higher alcohols. In contrast, $\Delta G_{\text{Excl}-\text{Vol}}$ decreases monotonically with alcohol concentration for both coil and globule polymer states (Fig. 2a, b). These trends have also been observed for aggregates of methane molecules in water-methanol mixtures[39]. This indicates that the hypothesis involving the strengthening of interactions in the bulk mixture does not apply to amphiphilic cosolvents such as methanol and ethanol. Note that the reversible work of cavity creation decreases at a faster rate for both coil and globule states in water–ethanol (Fig. 2b) mixtures as compared to water–methanol mixtures (Fig. 2a). These trends in $\Delta G_{\text{Excl}-\text{Vol}}$ correlate with the trends in surface tension of water-alcohol solutions[51], indicating that a macroscopic thermodynamic description applies in macromolecular solvation.

Discussion

The decrease in the reversible work of cavity creation in the presence of amphiphilic cosolvents such as methanol and ethanol is caused by preferential adsorption of the cosolvent on the polymer surface (see Supplementary Figs. 4–6 in Supplementary Note 2). The corresponding screening of the hydrophobic polymer–water interface by these alcohols reduces its unfavorable interaction with water, thereby reducing the free energy of the non-polar surface. However, a loss of cosolvent translational entropy in the bulk accompanies the preferential accumulation of the cosolvent. Therefore, the extent of screening or decrease in the free energy of the non-polar surface is determined by interplay between these two effects, which depends on the bulk cosolvent concentration. At low cosolvent concentration, the

globule state, due to its compact nature and lower SASA, can be more readily screened by the cosolvent than the coil state (see schematic in Fig. 2c). This leads to a higher preferential adsorption of the alcohol to the globule state than to the expanded coil state which in turn leads to a faster decrease in $\Delta G_{\text{Excl}-\text{Vol}}^{\text{G}}$ (Fig. 2a, b) thereby providing the driving force that shifts the polymer coil–globule equilibrium towards the globule state. This dependence of $\Delta G_{\text{Excl}-\text{Vol}}$ on the alcohol concentration can also be observed in the calculations of the reversible work of cavity creation for poly(N-isopropylacrylamide) (PNIPAM) in water-methanol mixtures[16] (see Supplementary Fig. 8 in Supplementary Note 3). Two important observations emerge from the results in Figs. 1b and 2. First, the concentration, $X_{\text{c,min}}$, corresponding to the minimum in $\Delta G_{\text{Excl}-\text{Vol}}^{\text{C}\rightarrow\text{G}}$, correlates with the concentration at which the globule state surface is saturated by the cosolvent (green markers in Fig. 2a, b). Second, the depth of the minimum in $\Delta G_{\text{Excl}-\text{Vol}}^{\text{C}\rightarrow\text{G}}$ is dependent on the difference between the rates of decrease in $\Delta G_{\text{Excl}-\text{Vol}}$ for the coil and the globule states (arrows in Fig. 2a, b). As this difference increases, the minimum in $\Delta G_{\text{Excl}-\text{Vol}}^{\text{C}\rightarrow\text{G}}$ becomes deeper. From Fig. 2b, it can be seen that the reversible work of cavity creation decreases, for both coil and globule states, at a faster rate in water-ethanol mixtures as compared to water–methanol mixtures. This occurs because, at the same alcohol concentration, ethanol can screen the surface more effectively than methanol due to its larger size. As a result, $X_{\text{c,min}}$ corresponds to a lower alcohol concentration for the higher alcohol (see green markers in Fig. 2a, b). These trends correlate with the observation that the surface tension of alcohol–water mixtures decreases at a higher rate for higher alcohols[51] and explain the cononsolvency behavior in PNIPAM–water–alcohol mixtures[8,19,48].

The trends in Fig. 2 furthermore rationalize the polymer molecular weight (or degree of polymerization N) dependence of the cononsolvency in PNIPAM-water-methanol mixtures where the minimum in LCST becomes deeper and shifts to higher methanol concentration with increase in N[46,47]. For both the coil and the globule states, the SASA increases with increase in N, with the rate of increase being higher for the former (SASA$^{\text{C}} \sim N^{\alpha_{\text{C}}}$, SASA$^{\text{G}} \sim N^{\alpha_{\text{G}}}$, $\alpha_{\text{C}} > \alpha_{\text{G}}$, see Supplementary Note 4). Due to the larger SASA, a higher cosolvent concentration is required for saturating the globular (and coiled) surface which in turn leads to an increase in $X_{\text{c,min}}$ (green markers in Fig. 3). Further, the difference between the rates of decrease in $\Delta G_{\text{Excl}-\text{Vol}}$ for the coil and globule states rises with N (arrows in Fig. 3), as the SASA of the former grows (with N) faster than the latter, due to which the minimum in $\Delta G_{\text{Excl}-\text{Vol}}^{\text{C}\rightarrow\text{G}}$ becomes deeper. Therefore, the minimum in $\Delta G_{\text{Excl}-\text{Vol}}^{\text{C}\rightarrow\text{G}}$, and in turn the LCST, becomes deeper and shifts to higher cosolvent concentration with increase in the molecular weight (right panel of Fig. 3). Note that one would expect similar trends with increase in the size of the monomer as well.

Interestingly, we find that the solvent–excluded volume of the polymer is not the only factor that determines the polymer collapse. The attractive polymer–cosolvent interactions are also found to play a crucial role, as reflected in the shift of the minima in $\Delta G^{\text{C}\rightarrow\text{G}}$ (and R_{g}) as a function of the strength of the polymer–alcohol attractions (see Fig. 4). Note that $\Delta G_{\text{Excl}-\text{Vol}}^{\text{C}\rightarrow\text{G}}$ is very weakly dependent on λ_{pa} as the polymer interacts with the solvent/cosolvent mixture through the WCA potential (see Supplementary Fig. 10 in Supplementary Note 5). Strengthening of the polymer–methanol attractive interactions (increasing λ_{pa}) shifts the polymer coil–globule equilibrium towards the expanded coil state, thereby reducing the concentration range where the collapsed state is thermodynamically favorable, $\Delta G^{\text{C}\rightarrow\text{G}} < 0$ (shaded regions in Fig. 4b). We attribute this trend to be the reason behind the experimentally observed absence of cononsolvency in poly(N,N-
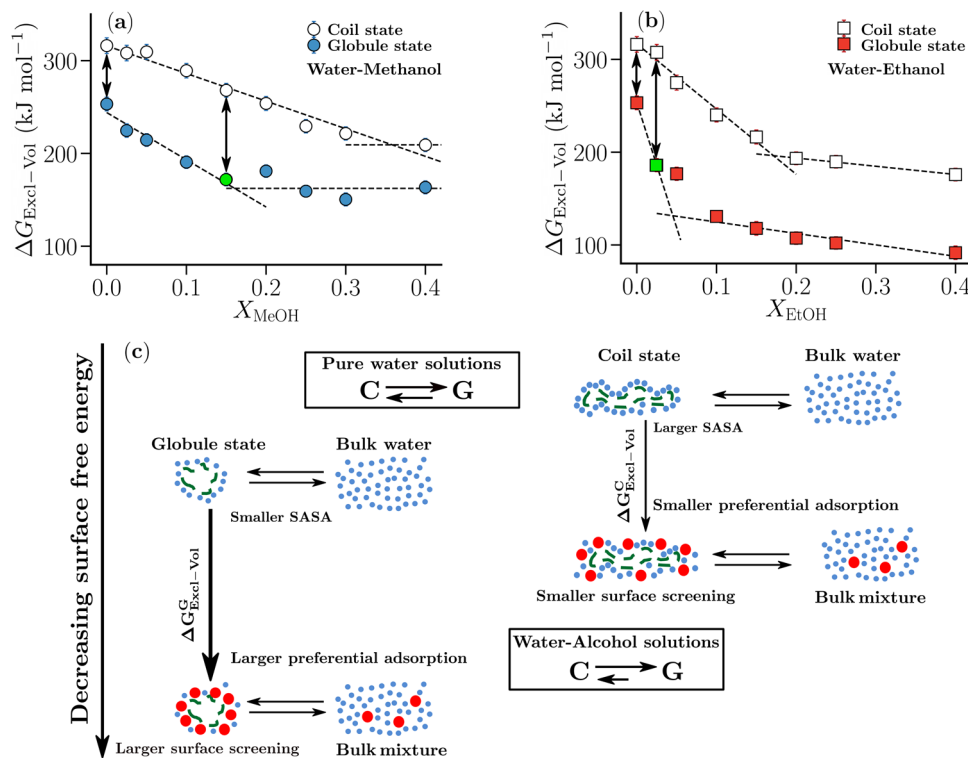
Fig. 2 Surfactant like behavior of alcohols favors polymer collapse. Dependence of the reversible work of cavity creation ($\Delta G^C_{Excl-Vol}$, $\Delta G^G_{Excl-Vol}$) for most probable coil and globule conformations on **a** methanol concentration X_{MeOH} and **b** ethanol concentrations X_{EtOH} for λ_{pa}=0.949. The green markers indicate the concentrations at which the globule state is nearly saturated by methanol and ethanol, and the dashed lines are linear fits for visual aid. **c** Schematic: the trade-off between polymer surface screening and cosolvent translational entropy in bulk determines the decrease in the surface free energy, $\Delta G_{Excl-Vol}$, for the coil and the globule states. The globule state, due to its compact size and lower SASA, can be more readily screened by cosolvent (larger preferential adsorption) than the coil state due to which its surface free energy, $\Delta G^G_{Excl-Vol}$, decreases faster than that of the coil state ($\Delta G^C_{Excl-Vol}$). The arrows in **a** and **b** show this difference between the rates of decrease in $\Delta G_{Excl-Vol}$ for the coil and the globule states. The reversible work of cavity creation decreases for both states at a faster rate for water-ethanol mixtures as, for the same concentration, ethanol can screen the polymer surface more effectively due to its larger size (green marker shifts to lower alcohol concentration as one moves from methanol to ethanol). For these simulations, λ_{pw} = 1.095 and λ_{pa} = 0.949. The error bars represent the standard errors in the respective quantities.

diethylacrylamide) (PDEA)–water–methanol mixtures[14,19,31,52]. Since PDEA has a larger non-polar surface area than PNIPAM[28], the PDEA–methanol van der Waals interaction (relative to PDEA–water interaction) would be stronger than PNIPAM–methanol interaction (relative to PNIPAM–water interaction). For a fixed polymer–water interaction strength (λ_{pw} = 1.095), it is expected that strengthening of the polymer–methanol attractive strength (increase in λ_{pa}) would lead to an increase in the preferential adsorption of methanol. This preferential adsorption, driven by the stronger polymer–cosolvent attractive interactions, shifts the polymer coil–globule equilibrium towards the coil state in the system studied herein (see Fig. 4). On the other hand, the preferential adsorption on the repulsive polymer surface due to the surfactant-like behavior of amphiphilic cosolvents (Fig. 1b) shifts the polymer coil–globule equilibrium towards the globule state. From Supplementary Figs. 4-7, it can be seen that the extent of preferential alcohol adsorption on the repulsive polymer surface (surfactant like behavior) is higher than that of the fully interacting polymer (see Supplementary Note 2 for more details). This clearly shows the prominent role played by the excluded volume interactions in driving the preferential accumulation of the cosolvent onto the polymer surface. We note that for strongly interacting co-solutes such as guanidinium thiocyanate salt and urea, attractive interactions lead to polymer collapse[7,13,20,28,53]. Therefore, depending on the underlying microscopic interactions, preferential cosolvent adsorption can either lead to polymer collapse or expansion. This may be the

reason for the inability of generic models[15,54], based only on preferential adsorption, to explain the differences between the behavior in PNIPAM and PDEA solutions. These observations indicate that cononsolvency depends on the interplay between the solvent–excluded-volume interactions, originating from bulk solvent–cosolvent interactions[8,44,55], and the polymer–solvent/cosolvent attractive interactions[5,13,14,33,34,41].

In conclusion, we showed that the polymer coil–globule equilibrium is governed by the interplay of solvent–excluded-volume interactions (free energy cost of creating a repulsive polymer–solvent interface) and polymer–solvent/cosolvent attractive van der Waals interactions. Our results demonstrate that amphiphilic cosolvents, such as methanol and ethanol, reduce the free energy cost of creating a repulsive polymer–solvent interface through a surfactant mechanism which surprisingly shifts the coil–globule equilibrium towards the collapsed globule state at low alcohol concentrations. The surfactant mechanism found herein is generic and should have important consequences for the physical properties of a wide variety of macromolecular systems. This is evident from the observation that the proposed interplay is able to rationalize the cononsolvency phenomenon of acrylamide polymers, and its dependence on the cosolvent size and polymer molecular weight.
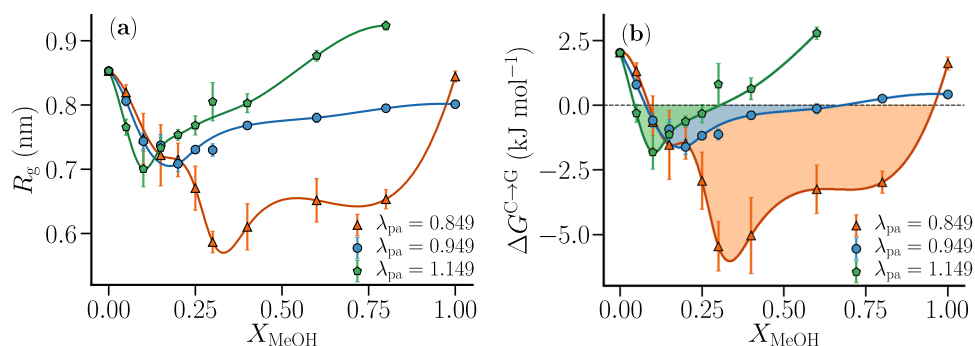
Methods
System details. We used a generic hydrophobic polymer model developed by Zangi et al.[56] consisting of 32 uncharged Lennard-Jones beads with σ_p = 0.4 nm

and $\epsilon_p = 1.0$ kJ mol^{-1}. The angular and bonded force-field parameters were taken from the same reference[56]. The aqueous polymer solution consisted of 5000 SPC/E[57] water molecules in a cubic box and the aqueous alcohol polymer solutions were described with the OPLS-UA force-field for methanol and ethanol (5000 molecule water-alcohol mixture)[58]. The generic polymer used in this work features a two-state conformational equilibrium C $\rightleftharpoons$ G, between coil (C) and globule (G) states[56]. Investigating cononsolvency for such a polymer model circumvents the sampling bottlenecks associated with atomistic models of real polymer systems such as of PNIPAM[33,59–61]. Our previous work showed that this model represents a poor solvent condition at 300 K and 1 atm, i.e., it provides a negative polymer collapse free energy of approximately -2 kJ mol^{-1} in SPC/E water[62]. To achieve good solvent conditions, the polymer–solvent interaction parameters (polymer–alcohol, ϵ_{pa} and polymer–water, ϵ_{pw}) were tuned while keeping the Lennard–Jones diameters (σ_{pa} and σ_{pw}) unchanged compared to the original model. The unlike interactions were described with Lorentz–Berthelot mixing rules. The polymer–solvent/cosolvent interaction parameter was scaled using a parameter λ_{px}, such that the $\epsilon_{px}^{new} = \lambda_{px}\epsilon_{px}$, where x is either alcohol (a) or water (w). The λ_{px} values were tuned to achieve positive collapse free energies in pure
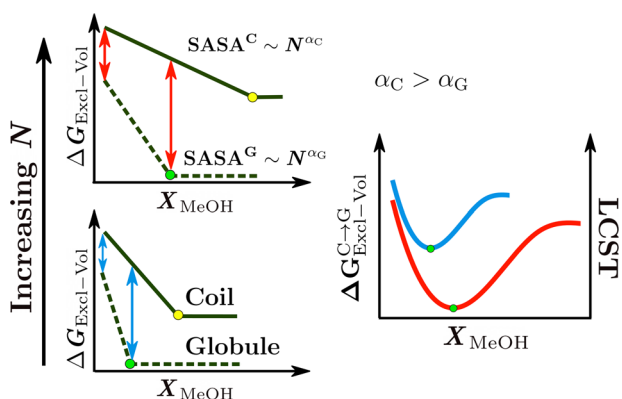
Fig. 3 Dependence of cononsolvency on the polymer molecular weight. Schematic showing the dependence of the reversible work of cavity creation for the coil and globule states on the degree of polymerization N and its correlation to the LCST dependence in PNIPAM-water-methanol solutions[46,47]. The SASAs of both coil and globule states grow with increase in N due to which the methanol concentration required to saturate them also increases (green and yellow markers in the left panel). As the SASA of the coil state (SASA$^C \sim N^{\alpha_C}$) grows faster with N than that of the globule (SASA$^G \sim N^{\alpha_G}$) state, $\alpha_C > \alpha_G$, the difference between the rates of decrease in $\Delta G_{Excl-Vol}$ for the coil and globule states rises with N (arrows in the left panel). These are the two aspects due to which the minimum in $\Delta G_{Excl-Vol}^{C\rightarrow G}$, and thereby the LCST, becomes deeper and shifts to higher methanol concentration with increase in N. The blue and red curves in the right panel represent the dependence of $\Delta G_{Excl-Vol}^{C\rightarrow G}$ (and LCST) on X_{MeOH} for the two chain lengths on the left panel.

water and pure alcohol (methanol and ethanol) systems (see Supplementary Figs. 1–3). The λ_{px} values used for the pure solvent systems and the alcohol-water mixtures were $\lambda_{pw} = 1.095$ for water, and $\lambda_{pa} = 0.949$ for methanol and ethanol. To study the effect of polymer–cosolvent interaction parameters, additional simulations were performed with $\lambda_{pa} = 0.849, 1.149$ for the polymer in water–methanol solutions.

Umbrella Sampling. Potential of mean force (PMF) profiles, $w(R_g)$, of the polymer in different methanol–water and ethanol–water mixtures were computed by carrying out umbrella sampling simulations with the GROMACS (version 4.6.7) package[63] using the PLUMED 2.2.0 plugin[64] and the polymer radius of gyration (R_g) as the collective variable. The harmonic restrain potential, $V(R_g)$, applied on the radius of gyration has the following form,

$$V(R_g) = \frac{k_b}{2}\left(R_g - R_g^o\right)^2, \qquad (1)$$

where $k_b (= 20000$ kJ mol^{-1}nm^2) is the force constant and R_g^o is the desired value of the radius of gyration. The collapsed and extended conformations of the polymer were determined using the two distinct minima in the PMF profiles below and above $R_g^\# = 0.7$ nm, respectively. Polymer conformations were sampled for R_g values between 0.4 nm and 1.2 nm with a spacing of $\Delta R_g = 0.025$ nm between successive windows. The equilibration and production runs for each window were performed in the NPT ensemble for 1 ns and 20 ns, respectively. For both the equilibration and production runs, the Nosé–Hoover thermostat[65,66] ($\tau_T = 0.5$ ps) and Parrinello–Rahman barostat[67] ($\tau_P = 1$ ps) were used. A 2 fs time step was used for the integration of the equations of motion. The Van der Waals interactions were truncated at 1.4 nm. Long-range Coulombic interactions were calculated with Particle Mesh Ewald[68] using a 1.4 nm real-space cutoff and a 0.12 nm grid spacing. The unbiased PMF was obtained using the weighted histogram analysis method (WHAM)[69]. The free energy change on polymer collapse, $\Delta G^{C\rightarrow G}$ was computed using,

$$e^{-\Delta G^{C\rightarrow G}/RT} = \frac{\int_0^{R_g^\#} e^{-w(R_g)/RT}dR_g}{\int_{R_g^\#}^\infty e^{-w(R_g)/RT}dR_g} \qquad (2)$$

where R is the gas constant, T is the temperature and R_g is the radius of gyration, $R_g^\# = 0.7$ nm is the cutoff for the R_g to determine the coil and the globule states of the polymer.

Thermodynamic integration. The reversible work of cavity formation for the coil and globule states was calculated using the thermodynamic integration (TI) method implemented in Gromacs (version 2019.3)[63] at different alcohol (methanol and ethanol) concentrations on the most probable coil ($R_g = 1.0$ nm) and globule ($R_g = 0.5$ nm) configurations. Position restraints, involving a harmonic potential with a force constant of 10^5 kJ mol^{-1} nm^{-2}, were applied on each polymer atom to keep the chain conformations fixed. In these TI calculations, polymer–water and polymer–alcohol WCA interactions[49] were slowly introduced. A leapfrog stochastic dynamics integrator[70] with an inverse friction constant of 0.1 ps was used for integrating the Newton's equations of motion and for maintaining the temperature of the system at 300 K. A total of 21 λ values with a spacing of 0.05 for $0 \le \lambda \le 1.0$ were used. The state $\lambda = 0$ corresponds to the cavity-free binary solvent. A soft-core potential with soft-core parameters $\alpha = 0.5$, $p = 1$ and $\sigma = 0.3$ nm was used to avoid singularities at the end state[71]. For each λ value, the energy of the system was minimized using the steepest descent algorithm. The equilibration process consisted of a 50 ps NVT run followed by a 100 ps NPT simulation (Berendsen

Fig. 4 Role of polymer–methanol attractive interactions in cononsolvency. Dependence of **a** radius of gyration R_g, and **b** polymer collapse free energy $\Delta G^{C\rightarrow G}$, on the methanol concentration X_{MeOH} for different λ_{pa} values. The concentration range over which the globule is thermodynamically favored, $\Delta G^{C\rightarrow G} < 0$, decreases with increase in the polymer–methanol attractive strength. It is expected that the preferential adsorption of methanol on the polymer would increase as the polymer–methanol attractive interaction strengthens. This increasing preferential adsorption shifts the polymer coil–globule equilibrium towards the coil state. This shows that preferential adsorption can favor either swelling or collapse of the polymer depending on the underlying microscopic interactions. For the above calculations $\lambda_{pw} = 1.095$. The error bars represent the standard errors in the respective quantities.

barostat[72], τ_p=1 ps). This was followed by a 5 ns production run (Parrinello–Rahman barostat, τ_p=1 ps) in which the first 200 ps were discarded.

Data availability

References

1. Maffi, C., Baiesi, M., Casetti, L., Piazza, F. & De Los Rios, P. First-order coil-globule transition driven by vibrational entropy. *Nat. Commun.* **3**, 1065 (2012).
2. Tiktopulo, E. I. et al. "Domain" coil-globule transition in homopolymers. *Macromolecules* **28**, 7519–7524 (1995).
3. Stuart, M. A. C. et al. Emerging applications of stimuli-responsive polymer materials. *Nat. Mater.* **9**, 101–113 (2010).
4. Bischofberger, I., Calzolari, D. C. E., De Los Rios, P., Jelezarov, I. & Trappe, V. Hydrophobic hydration of poly-N-isopropyl acrylamide: a matter of the mean energetic state of water. *Sci. Rep.* **4**, 4377 (2014).
5. Schild, H. G., Muthukumar, M. & Tirrell, D. A. Cononsolvency in mixed aqueous solutions of poly(N-isopropylacrylamide). *Macromolecules* **24**, 948–952 (1991).
6. Wang, J., Liu, B., Ru, G., Bai, J. & Feng, J. Effect of urea on phase transition of poly(N-isopropylacrylamide) and poly(N,N-diethylacrylamide) hydrogels: A clue for urea-induced denaturation. *Macromolecules* **49**, 234–243 (2016).
7. Sagle, L. B. et al. Investigating the hydrogen-bonding model of urea denaturation. *J. Am. Chem. Soc.* **131**, 9304–9310 (2009).
8. Bischofberger, I., Calzolari, D. C. E. & Trappe, V. Co-nonsolvency of PNiPAM at the transition between solvation mechanisms. *Soft Matter* **10**, 8288–8295 (2014).
9. Zhang, Y., Furyk, S., Bergbreiter, D. E. & Cremer, P. S. Specific ion effects on the water solubility of macromolecules: PNIPAM and the Hofmeister series. *J. Am. Chem. Soc.* **127**, 14505–14510 (2005).
10. Zhang, Y. et al. Effects of Hofmeister anions on the LCST of PNIPAM as a function of molecular weight. *J. Phys. Chem. C* **111**, 8916–8924 (2007).
11. Zhang, Y. & Cremer, P. S. Chemistry of Hofmeister anions and osmolytes. *Annu. Rev. Phys. Chem.* **61**, 63–83 (2010).
12. Cho, Y. et al. Effects of Hofmeister anions on the phase transition temperature of elastin-like polypeptides. *J. Phys. Chem. B* **112**, 13765–13771 (2008).
13. Heyda, J., Muzdalo, A. & Dzubiella, J. Rationalizing polymer swelling and collapse under attractive cosolvent conditions. *Macromolecules* **46**, 1231–1238 (2013).
14. Hofmann, C. H., Plamper, F. A., Scherzinger, C., Hietala, S. & Richtering, W. Cononsolvency revisited: solvent entrapment by N-isopropylacrylamide and N,N-diethylacrylamide microgels in different water/methanol mixtures. *Macromolecules* **46**, 523–532 (2013).
15. Mukherji, D. & Kremer, K. Coil-globule-coil transition of PNIPAm in aqueous methanol: coupling all-atom simulations to semi-grand canonical coarse-grained reservoir. *Macromolecules* **46**, 9158–9163 (2013).
16. Rodríguez-Ropero, F., Hajari, T. & Van der Vegt, N. F. A. Mechanism of polymer collapse in miscible good solvents. *J. Phys. Chem. B* **119**, 15780–15788 (2015).
17. Kyriakos, K. et al. Solvent dynamics in solutions of PNIPAM in water/methanol mixtures-a quasi-elastic neutron scattering study. *J. Phys. Chem. B* **120**, 4679–4688 (2016).
18. Walter, J., Sehrt, J., Vrabec, J. & Hasse, H. Molecular dynamics and experimental study of conformation change of poly(N-isopropylacrylamide) hydrogels in mixtures of water and methanol. *J. Phys. Chem. B* **116**, 5251–5259 (2012).
19. Liu, B., Wang, J., Ru, G., Liu, C. & Feng, J. Phase transition and preferential alcohol adsorption of poly(N,N-diethylacrylamide) gel in water/alcohol mixtures. *Macromolecules* **48**, 1126–1133 (2015).
20. Heyda, J. et al. Guanidinium can both cause and prevent the hydrophobic collapse of biomacromolecules. *J. Am. Chem. Soc.* **139**, 863–870 (2017).
21. Okur, H. I. et al. Beyond the Hofmeister series: Ion-specific effects on proteins and their biological functions. *J. Phys. Chem. B* **121**, 1997–2014 (2017).
22. Bruce, E. E., Bui, P. T., Rogers, B. A., Cremer, P. S. & Van der Vegt, N. F. A. Nonadditive ion effects drive both collapse and swelling of thermoresponsive polymers in water. *J. Am. Chem. Soc.* **141**, 6609–6616 (2019).
23. Bruce, E. E. & Van der Vegt, N. F. A. Molecular scale solvation in complex solutions. *J. Am. Chem. Soc.* **141**, 12948–12956 (2019).
24. Mondal, J., Stirnemann, G. & Berne, B. J. When does trimethylamine N-oxide fold a polymer chain and urea unfold it? *J. Phys. Chem. B* **117**, 8723–8732 (2013).
25. Mondal, J. et al. How osmolytes influence hydrophobic polymer conformations: a unified view from experiment and theory. *Proc. Natl Acad. Sci. USA* **112**, 9270–9275 (2015).
26. Liao, Y.-T., Manson, A. C., DeLyser, M. R., Noid, W. G. & Cremer, P. S. Trimethylamine N-oxide stabilizes proteins via a distinct mechanism compared with betaine and glycine. *Proc. Natl Acad. Sci. USA* **114**, 2479–2484 (2017).
27. Rodríguez-Ropero, F. & Van der Vegt, N. F. A. Direct osmolyte-macromolecule interactions confer entropic stability to folded states. *J. Phys. Chem. B* **118**, 7327–7334 (2014).
28. Nayar, D., Folberth, A. & Van der Vegt, N. F. A. Molecular origin of urea driven hydrophobic polymer collapse and unfolding depending on side chain chemistry. *Phys. Chem. Chem. Phys.* **19**, 18156–18161 (2017).
29. Sapir, L. & Harries, D. Macromolecular compaction by mixed solutions: bridging versus depletion attraction. *Curr. Opin. Colloid Interface Sci.* **22**, 80 – 87 (2016).
30. Winnik, F. M., Ringsdorf, H. & Venzmer, J. Methanol-water as a co-nonsolvent system for poly(N-isopropylacrylamide). *Macromolecules* **23**, 2415–2416 (1990).
31. Maeda, Y., Nakamura, T. & Ikeda, I. Change in solvation of poly(N,N-diethylacrylamide) during phase transition in aqueous solutions as observed by ir spectroscopy. *Macromolecules* **35**, 10172–10177 (2002).
32. Jia, D. et al. Re-entrance of poly(N,N-diethylacrylamide) in D$_2$O/d-ethanol mixture at 27 °C. *Macromolecules* **49**, 5152–5159 (2016).
33. Dalgicdir, C., Rodríguez-Ropero, F. & Van der Vegt, N. F. A. Computational calorimetry of PNIPAM cononsolvency in water/methanol mixtures. *J. Phys. Chem. B* **121**, 7741–7748 (2017).
34. Okada, Y. & Tanaka, F. Cooperative hydration, chain collapse, and flat LCST behavior in aqueous poly(N-isopropylacrylamide) solutions. *Macromolecules* **38**, 4465–4471 (2005).
35. Sommer, J.-U. Adsorption-attraction model for co-nonsolvency in polymer brushes. *Macromolecules* **50**, 2219–2228 (2017).
36. Mochizuki, K., Pattenaude, S. R. & Ben-Amotz, D. Influence of cononsolvency on the aggregation of tertiary butyl alcohol in methanol-water mixtures. *J. Am. Chem. Soc.* **138**, 9045–9048 (2016).
37. Mochizuki, K. & Ben-Amotz, D. Hydration-shell transformation of thermosensitive aqueous polymers. *J. Phys. Chem. Lett.* **8**, 1360–1364 (2017).
38. Pica, A. & Graziano, G. An alternative explanation of the cononsolvency of poly(N-isopropylacrylamide) in water-methanol solutions. *Phys. Chem. Chem. Phys.* **18**, 25601–25608 (2016).
39. Mochizuki, K. & Koga, K. Cononsolvency behavior of hydrophobes in water + methanol mixtures. *Phys. Chem. Chem. Phys.* **18**, 16188–16195 (2016).
40. Chandler, D. Interfaces and the driving force of hydrophobic assembly. *Nature* **437**, 640–647 (2005).
41. Mukherji, D., Marques, C. M. & Kremer, K. Polymer collapse in miscible good solvents is a generic phenomenon driven by preferential adsorption. *Nat. Commun.* **5**, 4882 (2014).
42. Sommer, J.-U. Gluonic and regulatory solvents: a paradigm for tunable phase segregation in polymers. *Macromolecules* **51**, 3066–3074 (2018).
43. Dudowicz, J., Freed, K. F. & Douglas, J. F. Communication: cosolvency and cononsolvency explained in terms of a Flory-Huggins type theory. *J. Chem. Phys.* **143**, 131101 (2015).
44. Bharadwaj, S., Kumar, P. B. S., Komura, S. & Deshpande, A. P. Kosmotropic effect leads to LCST decrease in thermoresponsive polymer solutions. *J. Chem. Phys.* **148**, 084903 (2018).
45. Budkov, Y. A., Kolesnikov, A. L., Georgi, N. & Kiselev, M. G. A statistical theory of cosolvent-induced coil-globule transitions in dilute polymer solution. *J. Chem. Phys.* **141**, 014902 (2014).
46. Scherzinger, C., Schwarz, A., Bardow, A., Leonhard, K. & Richtering, W. Cononsolvency of poly-N-isopropyl acrylamide (PNIPAM): microgels versus linear chains and macrogels. *Curr. Opin. Colloid Interface Sci.* **19**, 84–94 (2014).
47. Tanaka, F., Koga, T., Kojima, H., Xue, N. & Winnik, F. M. Preferential adsorption and co-nonsolvency of thermoresponsive polymers in mixed solvents of water/methanol. *Macromolecules* **44**, 2978–2989 (2011).
48. Wang, N., Ru, G., Wang, L. & Feng, J. 1h mas nmr studies of the phase separation of poly(N-isopropylacrylamide) gel in binary solvents. *Langmuir* **25**, 5898–5902 (2009).
49. Weeks, J. D., Chandler, D. & Andersen, H. C. Role of repulsive forces in determining the equilibrium structure of simple liquids. *J. Chem. Phys.* **54**, 5237–5247 (1971).
50. Onori, G. Adiabatic compressibility and structure of aqueous solutions of ethyl alcohol. *J. Chem. Phys.* **89**, 4325–4332 (1988).

51. Xu, L. et al. Hydrophobic coating- and surface active solvent-mediated self-assembly of charged gold and silver nanoparticles at water-air and water-oil interfaces. *Phys. Chem. Chem. Phys.* **11**, 6490–6497 (2009).

52. Scherzinger, C., Lindner, P., Keerl, M. & Richtering, W. Cononsolvency of poly(N,N-diethylacrylamide) (PDEAAM) and poly(N-isopropylacrylamide) (PNIPAM) based microgels in water/methanol mixtures: copolymer vs core-shell microgel. *Macromolecules* **43**, 6829–6833 (2010).

53. Micciulla, S. et al. Concentration dependent effects of urea binding to poly(N-isopropylacrylamide) brushes: a combined experimental and numerical study. *Phys. Chem. Chem. Phys.* **18**, 5324–5335 (2016).

54. Yong, H., Merlitz, H., Fery, A. & Sommer, J.-U. Polymer brushes and gels in competing solvents: the role of different interactions and quantitative predictions for poly(N-isopropylacrylamide) in alcohol-water mixtures. *Macromolecules* **53**, 2323–2335 (2020).

55. Bharadwaj, S. & Van der Vegt, N. F. A. Does preferential adsorption drive cononsolvency? *Macromolecules* **52**, 4131–4138 (2019).

56. Zangi, R., Zhou, R. & Berne, B. J. Urea's action on hydrophobic interactions. *J. Am. Chem. Soc.* **131**, 1535–1541 (2009).

57. Berendsen, H. J. C., Grigera, J. R. & Straatsma, T. P. The missing term in effective pair potentials. *J. Phys. Chem.* **91**, 6269–6271 (1987).

58. Jorgensen, W. L. Optimized intermolecular potential functions for liquid alcohols. *J. Phys. Chem.* **90**, 1276–1284 (1986).

59. Kang, Y., Joo, H. & Kim, J. S. Collapse-swelling transitions of a thermoresponsive, single Poly(N-isopropylacrylamide) chain in water. *J. Phys. Chem. B* **120**, 13184–13192 (2016).

60. Dalgicdir, C. & Van der Vegt, N. F. A. Improved temperature behavior of PNIPAM in water with a modified OPLS model. *J. Phys. Chem. B* **123**, 3875–3883 (2019).

61. Garcìa, E. J. & Hasse, H. Studying equilibria of polymers in solution by direct molecular dynamics simulations: Poly(N-isopropylacrylamide) in water as a test case. *Eur. Phys. J.* **227**, 1547–1558 (2019).

62. Nayar, D. & Van der Vegt, N. F. A. Cosolvent effects on polymer hydration drive hydrophobic collapse. *J. Phys. Chem. B* **122**, 3587–3595 (2017).

63. Abraham, M. J. et al. Gromacs: High performance molecular simulations through multi-level parallelism from laptops to supercomputers. *SoftwareX* **1-2**, 19–25 (2015).

64. Tribello, G. A., Bonomi, M., Branduardi, D., Camilloni, C. & Bussi, G. Plumed 2: New feathers for an old bird. *Comput. Phys. Commun.* **185**, 604 – 613 (2014).

65. Nosé, S. A unified formulation of the constant temperature molecular dynamics methods. *J. Chem. Phys.* **81**, 511–519 (1984).

66. Hoover, W. G. Canonical dynamics: equilibrium phase-space distributions. *Phys. Rev. A* **31**, 1695 (1985).

67. Parrinello, M. & Rahman, A. Polymorphic transitions in single crystals: a new molecular dynamics method. *J. Appl. Phys.* **52**, 7182–7190 (1981).

68. Darden, T., York, D. & Pedersen, L. Particle mesh ewald: An $N\log(N)$ method for ewald sums in large systems. *J. Chem. Phys.* **98**, 10089–10092 (1993).

69. Kumar, S., Rosenberg, J. M., Bouzida, D., Swendsen, R. H. & Kollman, P. A. Multidimensional free-energy calculations using the weighted histogram analysis method. *J. Comput. Chem.* **16**, 1339–1350 (1995).

70. Gunsteren, W. F. V. & Berendsen, H. J. C. A leap-frog algorithm for stochastic dynamics. *Mol. Simul.* **1**, 173–185 (1988).

71. Pham, T. T. & Shirts, M. R. Identifying low variance pathways for free energy calculations of molecular transformations in solution phase. *J. Chem. Phys.* **135**, 034114 (2011).

72. Berendsen, H. J. C., Postma, J. P. M., Van Gunsteren, W. F., DiNola, A. & Haak, J. R. Molecular dynamics with coupling to an external bath. *J. Chem. Phys.* **81**, 3684–3690 (1984).

Author contributions

S.B., D.N., and C.D. contributed equally to this work. All authors were involved in designing the research and analysis of data. D.N. and C.D. performed the umbrella sampling simulations. S.B. performed the thermodynamic integration simulations. S.B., D.N., and N.v.d.V. wrote the paper.

Funding

Competing interests

The authors declare no competing interests.

Additional information

Supplementary information is available for this paper at https://doi.org/10.1038/s42004-020-00405-x.

Correspondence and requests for materials should be addressed to S.B. or N.F.A.v.d.V.

Reprints and permission information is available at http://www.nature.com/reprints

Publisher's note Springer Nature remains neutral with regard to jurisdictional claims in published maps and institutional affiliations.